IONIZATION OF NO AT HIGH TEMPERATURE

Final Report on Phase I of NASA Grant NAG-1-1211,
January 1991-November 1991, with the
University of Oregon

Submitted by
Prof. C. Frederick Hansen, Principal Investigator
Chemical Physics Institute
University of Oregon
Eugene, Oregon, 97403

IONIZATION OF NO AT HIGH TEMPERATURE*

C. Frederick Hansen**

INTRODUCTION

Space vehicles flying through the atmosphere at high speed are known to excite a complex set of chemical reactions in the atmospheric gases, ranging from simple vibrational excitation to dissociation, atom exchange, electronic excitation, ionization, and charge exchange. The major reactions in high temperature air were measured in the 1960's, generally in shock tubes, at temperatures up to about 10000°K; and Arrhenius type equations were then fit to the observed rate coefficients. Although rate data is typically rather scattered, even for measurements made with a fixed experimental arrangement--and different experiments often yield widely different results--yet for some engineering purposes the uncertainties are not excessive. This occurs because endothermic rate coefficients, at least, change so rapidly with temperature that in flow field calculations where temperature gradients are high, as they are in the blunt body regions or boundary layer regions of high velocity vehicle flow, the uncertainties in the rate coefficient have a minor effect on species concentration and thermodynamic properties as a function of distance along the flow.

However, the exothermic rate coefficients can introduce significant uncertainties in cooler regions of flow such as the inner boundary layers adjacent to the body surface or in the expansion flow along the aft part of the vehicle and in the vehicle's wake. Moreover, the rate coefficients are now needed at much higher temperature and lower density than formerly, for application to the new class of space vehicles planned, such as the AOTV--Aeroassisted Orbit Transfer Vehicle. Temperatures up to 40000°K are well beyond the range that seems accessible to experiment and extrapolation of the formulae which fit the lower temperature data is uncertain unless a theoretical model can be devised to justify the extrapolation. Finally, the new class of space vehicles will decelerate at very high altitude (more than 60 km. above the earth's surface) where the density is so low that the shock heated gases will often not be in either thermal or chemical equilibrium. Since most of the measured reaction rates have been made at conditions where equilibrium is believed to obtain, a theoretical model is also desired which can treat particularly the effects of vibrational and electronic nonequilibrium on the rate processes.

The purpose of this paper is to develop simple arguments for the temperature dependence of the reactions leading to ionization of NO, including the effect of vibrational-electronic thermal nonequilibrium. NO ionization is the most important source of electrons at intermediate temperatures and at higher temperatures

provides the trigger electrons that ionize atoms. Based on these arguments, recommendations will be made for formulae which fit observed experimental results, and which include a dependence on both a heavy particle temperature T and different vibration-electron temperatures T_v and T_e. In addition, these expressions will presumably provide the most reliable extrapolation of experimental results to much higher temperatures.

TEMPERATURE DEPENDENCE OF EXOTHERMIC AND ENDOTHERMIC REACTIONS

The rate coefficient for a two-body collision induced reaction can be expressed quite rigorously as the reaction cross section S times the collision velocity integrated over a Maxwell-Boltzmann distribution of collision energies[1].

$$k = \frac{\bar{u}}{s} \int_o^\infty S(x)\, x\, e^{-x}\, dx \qquad \text{Eq.(1)}$$

where $\bar{u}$ is the mean velocity of the collision pair in center of mass coordinates, s is the symmetry number--unity for dissimilar particles, two for similar particles, and x is the dimensionless collision energy in units of kT (i.e. $x = E/kT = \mu u^2/2kT$).

If the collision is exothermic with no activation energy, the cross section is expected to be a relatively slowly varying function of energy. For example, if the cross section varies inversely with the m^{th} power of collision energy

$$S = \frac{S_o}{E^m} = (kT)^{-m} \frac{S_o}{x^m} \qquad \text{Eq.(2)}$$

then the integral of Eq.(1) is analytic if $m < 2$

$$k_{exo} = \frac{\bar{u} S_o}{(kT)^m} \Gamma(1-m) \propto T^{-(m-1/2)} \qquad \text{Eq.(3)}$$

However, when the reaction is endothermic, the integration is performed over x only from x_o to infinity, or over all $y = (x - x_o)$, the dimensionless energy in excess of the threshold energy x_o.

$$k = \frac{\bar{u}}{s} \left[\int_o^\infty S(y)\, (x_o + y)\, e^{-y} dy \right] e^{-x_o} \qquad \text{Eq.(4)}$$

Eq.(4) is the form of the usual Arrhenius expression for endothermic reaction

$$k = C(T)\, e^{-E_o/kT} \qquad \text{Eq.(5)}$$

where the temperature dependence of the preexponential factor depends on the average collision velocity $\bar{u}$ and the definite integral determined by the shape of the cross section function S(y)

$$C(T) = \frac{\bar{u}}{s} \int_o^\infty S(y)\, (x_o+y)\, e^{-y}\, dy \qquad \text{Eq.(5a)}$$

An additional factor that needs be considered is that while highly excited electronic states do not contribute much to exothermic reaction because their population numbers decrease so rapidly, the endothermic reactions to not usually occur from the ground state but from excited electronic states that have activation energies the order of kT. The exponential decrease in population number of the excited state is balanced by the exponential increase in the rate coefficient due to the lower activation energy. The total rate coefficient is the sum of rate coefficients from each state i weighted by the probability that the i^{th} state is involved in the collision. This remains an expression like Eq.(5) with the same activation energy E_o

$$k = \sum_i k_i \left(\frac{n_i}{n}\right) = \frac{1}{Q} \sum_i g_i C_i(T)\, e^{-(E_o-E_i)/kT} e^{-E_i/kT} - \frac{1}{Q} \left(\sum_i g_i C_i(T)\right) e^{-E_o/kT} \qquad \text{Eq.(5b)}$$

where n_i and n are respectively the densities of the reactive molecule in the i^{th} state and the total number density of all states. The preexponential term is a sum of all the preexponential terms $C_i(T)$ weighted with the degeneracies g_i divided by the partition function Q; these sums may include all the rotational and vibrational states of internal energy as well as electronic states.

The temperature dependence of endothermic reaction is dominated by the exponential factor $\exp(-E_o/kT)$ whenever the activation energy E_o is large compared with kT. Then it is not possible to arrive at a good estimate for the temperature dependence of the preexponential term from experimental data because the slope of an Arrhenius plot of ln(k) as a function of 1/kT is very nearly $-E_o$ no matter what preexponential function is chosen. For example, an endothermic rate coefficient that has been widely used[2,3] for the heavy particle impact dissociation of O_2 is

$$k = \frac{3.74x10^{18}}{T} e^{-59400/T} \quad cc/mol\text{-}sec \qquad \text{Eq.(5c)}$$

However, as Fig.(1) shows, the slope of the Arrhenius plot is changed very little if the exponent on the preexponential temperature term is changed ±1/2. This particular example is chosen to illustrate the point because the data provided by Camac and Vaughan[2] on O_2 dissociation by Ar impact is about the least scattered data for high temperature endothermic reaction that has been obtained. Still enough scatter remains so that the least squares deviation is almost the same for any one of the three functions shown. In most cases the scatter in measured rate coefficients is much greater; thus the best way to arrive at the correct temperature dependence of rate coefficients is to determine the exothermic rate, if possible, and then calculate the endothermic rate with the equilibrium constant, which is a well known expression involving the partition functions of the chemically reacting species.

To develop the analysis further, the shape of the reactive cross section as a function of collision energy must be given, either as an experimentally measured parameter, or as a theoretical estimate.

REACTION CROSS SECTION THEORY

Various empirical or semiempirical approximations have been tried for the reactive cross section. Qualitatively the cross section must vanish at collision velocities less than the activation energy, then it increases rather rapidly as collision energy exceeds the threshold, maximizes at something less than the total scattering cross section, and finally decreases at much higher collision energies. Hansen[4] has suggested a cross section function for collision induced dissociation of O_2, N_2, and NO which increases as the square of the excess collision energy above threshold and eventually decreases as 1/E

$$\frac{S}{S_o} = 2(1-E_o/E)^2(E_o/E) \qquad \text{Eq.(6)}$$

This cross section is based on arguments that involve the conservation of angular momentum in repulsion and the assumption that the probability of no transition at the crossing of reactant and product potential surfaces increases linearly with collision energy in excess of the activation energy. The results are roughly similar to an empirical function proposed by Lotz[5] and recommended by Park[6]

$$\frac{S}{S_o} = \frac{\ln(E/E_o)}{E/E_o} \qquad \text{Eq.(7)}$$

This function has a shape similar to experimental measurement of H atom ionization[7] and N atom ionization[8] by electron impact. However both of these functions peak at much lower energies than required to agree with molecular ionization cross sections by heavy particle impact measured by Utterback[9] and Utterback and VanZyl[10].

Perhaps the most complete model of reactive cross sections presently available is due to Landau[11] and Zener[12]. A brief review of their theory will establish the basis for subsequent analysis in this paper. Transition from a reactant system to a product system is presumed to occur within a narrow range of intermolecular distance r_o where the potential surfaces of the reactant and product systems cross, or at least come very close to one another. The situation is diagrammed in Fig.(2) for repulsive potentials leading to endothermic reaction. The potential of the reactants at infinite separation is taken as the reference zero and the potential at the crossing point is E_o. This will also be the activation energy E^* if the potential surfaces are repulsive as shown on Fig.(2). However, if the potential of the product system should have a minimum, E^* can then be greater than E_o. The initial collision energy E is conserved and after the reaction the kinetic energy of the product species is E less the change in zero point energy of the chemical species involved. The product system potential is often only weakly repulsive, in which case the change in zero point energy, E°, and the activation, E^*, are about equal.

If q is the probability that transition does not occur as the system crosses the reaction zone, (1-q) is the probability that transition does occur. Then q(1-q) is the probability that transition does not occur during the incoming crossing but does occur outgoing. Similarly (1-q)q is the probability that transition occurs incoming and is not undone outgoing. Thus the total probability of transition during the collision is

$$P = q(1-q) + (1-q)q = 2q(1-q) \qquad \text{Eq.(8)}$$

Landau and Zener develop an exponential expression for q

$$q = \exp\left(\frac{-4\pi H_{12}^2}{u\hbar \left|\frac{d}{dr}(H_{11}-H_{22})\right|}\right) = e^{-a/u} \qquad \text{Eq.(9)}$$

where u is the velocity with which the system crosses the reaction zone and the matrix elements are the total Hamiltonian of the system averaged over the initial and/or final state wave functions

$$H_{ik} = \langle \phi_k^* |H| \phi_i \rangle \qquad \text{Eq.(10)}$$

H_{11} and H_{22} are just the potential surfaces of the reactant and product systems respectively. The gradients of these potentials and the interaction energy H_{12} are all evaluated at r_o. In general neither the potentials, nor their slopes, nor the interaction energy are known, but they are all constants which can be gathered in the parameter a in Eq.(9), a constant with the dimension of velocity. The assumptions used in the Landau-Zener treatment leave some doubt about the exact quantitative results in any case, but if the functional relations are reliable, the constant a can be established by comparison with measured reaction cross sections and/or measured rate coefficients wherever these are available.

The following analysis considers the special case where both reactant and product potentials are repulsive and spherically symmetric with the activation energy the same as the crossing potential E_o. If the collision is head on, that is with miss distance b equal zero, the crossing velocity u_o is $(2(E-E_o)/\mu)^{1/2}$, the velocity of the system in center of mass coordinates when it has slowed from the kinetic energy E at infinite separation to the remaining kinetic energy at the crossing region. However, practically all the collisions approach with miss distance somewhat greater than zero. The maximum miss distance b_m which allows the system to reach the reaction coordinate r_o is

$$\left(\frac{b_m}{r_o}\right)^2 = \left(1-\frac{E_o}{E}\right) \qquad \text{Eq.(11)}$$

This relation obtains because of conservation of angular momentum and does not depend on the shape of the repulsive interaction[1]. However at the maximum miss distance b_m the system just grazes the crossing surface with zero crossing velocity. At intermediate miss distances the crossing velocity will decrease monotonicly from u_o at b = 0, slowly at first, and then rapidly approach zero as b approaches b_m. The exact shape of the crossing velocity u(b) will depend on the shape of the repulsive potential. Whatever the exact shape may be, it should be possible to approximate the probability q(b) with a function of the type

$$q(b) = e^{-a/u(b)} \approx e^{-a/u_o[1-(b/b_m)^d]} \qquad \text{Eq.(12)}$$

where d is a constant coefficient chosen to fit the true relation.

The reaction cross section for the collision energy E can then be expressed

$$S(E) = 2\pi \int_{o}^{b_m} 2q(b)\,[1-q(b)]\,b\,db \approx 2\pi b_m^2 \left(\frac{d}{d+2} e^{-a/u_o} - \frac{d-1}{d+2} e^{-2a/u_o} \right) \qquad \text{Eq.(13)}$$

A slow decrease in q(b) is expected near b=0 in which case d should be considerably larger than unity. Then the integral of Eq.(13) is approximately independent of the coefficient d

$$\frac{S(E)}{S_o} = 2\,(1-E_o/E)\,[e^{-c/(E/E_o-1)^{1/2}} - e^{-2c/(E/E_o-1)^{1/2}}] \qquad \text{Eq.(13a)}$$

The constant S_o is πr_o^2 times the fraction of collisions that approach along the potential surface leading to transition. The dimensionless parameter c is related to the constant velocity parameter a

$$c = \left(\frac{\mu a^2}{2E_o} \right)^{1/2} \qquad \text{Eq.(13b)}$$

The object has been merely to establish a reasonable functional relation between the cross section and the collision energy. The constants S_o and c are simply chosen to agree with experimental data.

Fig.(3) shows the $\log(S/S_o)$ for the Landau-Zener form of cross section as a function of $\log(E/E_o)$ for a variety of the constants c equal to 1, 5, 10, 20, and 30. Wherever experimental values may be available, the maximum in the function can be established at the observed value by the choice of c; then the magnitude of the cross section is matched by the choice of S_o. In addition, Fig.(3) shows the more empirical functions proposed[4,6]. These more or less match the maximum given by the Landau-Zener model when c is a little less than unity, but they fall off much more rapidly for high energy collisions. This difference will not affect the integrations that provide the rate coefficient very much as long as temperature is small compared with E_o/k, but can make a difference at much higher temperature. Also shown on Fig.(3) are the measured cross sections for NO ionization by N_2 collision[9]. For this reaction, at least, a constant c about 10 is appropriate. Utterback finds some structure in this cross section, a very small hump near threshold, which no doubt indicates another reaction path. However this makes a negligible contribution to the rate coefficient integral and so is ignored here. The difference between the measurements and the

theoretical model is accentuated on the log plot; a better indication of the comparison between the two as far as the rate coefficient integral is concerned is a plot of S as a function of E/E_o as shown on Fig.(4). This figure shows the kind of fit to experiment that can be achieved with the Landau-Zener theory; in contrast, the empirical function $\ln(S/S_o)/(S/S_o)$ is seen to peak at collision energies far below the observed peak and to fall off much too rapidly at higher energies. The same is true of the function of Eq.(6). While those empirical functions may approximate realistic cross sections for electron impact ionization or for dissociation by heavy particle impact, they certainly do not provide good cross sections for ionization of NO by N_2 impact. The Landau-Zener model is a far more flexible function that can better fit experimental data, to say nothing of the confidence provided by the theoretical foundation for the function.

DISSOCIATIVE ELECTRON RECOMBINATION $NO^+ + e \rightarrow N + O$

The most important mechanism for ionization in air at moderately high temperature (the order of 5000°K or so) is the collision between N and O atoms

$$N + O \rightleftharpoons NO^+ + e \qquad \text{Eq.(14)}$$

Because of the importance of this reaction, numerous measurements of both the endothermic and exothermic rate coefficient have been made. However, the scatter in the data is severe as shown by the exothermic rates plotted on Figure (5). Thus some uncertainty still exists about the exact rates for the reaction.

The measured exothermic rate coefficients will be of most interest here because these have the best chance of providing the correct temperature dependence for the rates, as discussed above. The first high temperature evaluation of the exothermic rate was provided by Lin and Teare[13]. They found a $T^{-3/2}$ dependence of the exothermic rate, and chose the constant to agree with low temperature data of Doering and Mahan[14].

$$k_{exo} = \frac{1.8 \times 10^{21}}{T^{3/2}} \quad cc/mol\text{-}sec \qquad \text{Eq.(15a)}$$

Subsequent experiments[15-18] confirmed the low temperature result rather well as shown on Fig.(5) (estimates of Whitten and Poppoff[19] were based on upper atmosphere airglow measurements and probably are not as reliable as the laboratory measurements). However, except for some results reported by Daiber[20], the measured high temperature rates have generally been higher than Eq.(15a). Thompson[21] suggested that Lin and Teare's results should be increased by a factor of 3, and Frohm and DeBoer[22] observed that a

factor of 2 increase actually gives a better fit to Lin and Teare's original data. Results reported by Bascomb, et al[23] and by Stein, et al[24] appear to confirm the higher value.

Since Lin and Teare's exothermic rate was deduced from measurements of the endothermic process, the functional dependence could be in question, as shown previously. However, Dunn and Lordi[25] observed the electron recombination process directly in expanding flow from a high temperature shock tunnel. They confirmed the same temperature dependence but with a somewhat larger rate

$$k_{exo} = \frac{6.7 \pm 2.3 \times 10^{21}}{T^{3/2}} \quad cc/mol\text{-}sec \qquad \text{Eq.(15b)}$$

Extrapolation of this function to lower temperature lies above most of the data there. Hansen[26] argued that at low temperature the relation should change to a $T^{-1/2}$ dependence because of the dependence of the equilibrium constant on temperature. Although this argument was based on an endothermic rate calculated for a constant transition probability at the potential crossing for the NO^+ and N+O systems, which is unrealistic, the same change in the functional trend will be found for an approximate endothermic rate based on the Landau Zener model of reaction.

Two recommendations made by critical reviewers of rate data are shown by the dotted lines on Fig.(5). Bortner[27] reviewed the literature available before 1969 and recommended

$$k_{exo} = \frac{(1.5 \pm 2.9) \times 10^{21}}{T^{3/2}} \quad cc/mol\text{-}sec \qquad \text{Eq.(15c)}$$

Blottner[27] recommended a slightly different function

$$k_{exo} = \frac{1.8 \times 10^{19}}{T} \quad cc/mol\text{-}sec \qquad \text{Eq.(15d)}$$

which has been widely used in flow field calculations[3].

The discussion above is sufficient to indicate a considerable degree of uncertainty in the rate constants for Eq.(14), in part due to the large number of different experimental investigations of the reaction. In addition, an account of the effect of non-equilibrium on this reaction has not been derived. In the next section the Landau Zener model of reaction rates will be applied to the problem in an attempt to provide a theoretical basis for the temperature dependence of the rates and to include the effect of vibration and electronic nonequilibrium.

THEORETICAL MODEL FOR DISSOCIATIVE ELECTRON RECOMBINATION

The perturbation potentials for collision of an electron with an NO^+ ion are represented by the 3-dimensional schematic of Fig.(6). Potentials for the N+O repulsion and for the NO^+ attractive well, when the free electron is at infinity, are shown in the U vs. r plane, where r is the intermolecular separation between the N and O atoms or between nuclear centers in the vibrating NO^+ ion. The repulsive N+O potential is presumed to cross at the ion's potential minimum; then the activation energy for endothermic reaction is just the change in zero point chemical energy and the activation energy for exothermic reaction vanishes, which seems to be in accord with experimental observation. The electron approaching the ion with kinetic energy E_e is accelerated as it falls into the strong Coulomb attractive potential ($E_e - e^2/r_e$), which is drawn in the U vs. r_e plane; r_e is the distance between the electron and the ion. Eventually the electron experiences a strong repulsion as it encroaches on the space occupied by the ion's electrons. This slows the electron to its initial kinetic energy and opens the possibility of transition to the N+O system if the vibrational configuration of the ion is nearly at the potential crossing point r_o. Of course, electrons behave more like quantum waves than classical particles in collision. However, except for misrepresenting features like glory and rainbow effects, a classical treatment is expected to cut through the average of the quantum results.

Because of the large Coulomb attraction, the cross section which leads to a close enough encounter to permit transition is very large. The maximum miss distance b_m which allows the electron to come within some distance r^* needed (the order of a Bohr radius) varies about inversely with the original electron energy. This is given by Eq.(11) except that in this case the potential is attractive

$$\frac{S}{S^*} = \left(\frac{b_m}{r^*}\right)^2 = 1 + \frac{e^2}{r^* E_e} \approx \frac{e^2}{r^* E_e} \qquad \text{Eq.(11a)}$$

The electron velocities will be the order of 100 times larger than heavy particle velocities in the gas, so for most collisions the transition probabilities are expected to be small. Then the total probability of transition given by Eq.(8) is approximately inversely proportional to the electron's velocity

$$P \approx 2(1 - e^{-a/u_e}) \approx \frac{2a}{u_e} = \frac{const}{E_e^{1/2}} \qquad \text{Eq.(16)}$$

Although this approximation is violated at very low collision energies, these are relatively unimportant for exothermic reaction as they are weighted so lightly by the Boltzmann distribution of energies. Eqs. (11a) and (16) combine to give the functional relation for total cross section which is inversely proportional to the 3/2 power of the electron's kinetic energy

$$S \propto \frac{S}{S^*} P = \frac{const}{E_e^{3/2}} = \frac{const}{(kT_e)^{3/2}\, x^{3/2}} \qquad \text{Eq.(17)}$$

Then the rate coefficient for transition has the form

$$k = \bar{u} \int_o^\infty S\, x\, e^{-x}\, dx \propto \frac{1}{T_e} \int_o^\infty \frac{e^{-x}\, dx}{x^{1/2}} = \frac{const}{T_e} \qquad \text{Eq.(18)}$$

Eq.(18) gives the functional dependence of the rate coefficient for a favorable vibrational configuration of the NO^+ ion. The probability p_v that an ion in vibrational state v is within a small region δ near the bottom of its potential well, and thus within the reaction zone, is

$$p_v = \frac{\delta}{\tau u_v} = \left(\frac{\mu}{2v\hbar\omega}\right)^{1/2} \frac{\delta}{\tau} \qquad \text{Eq.(19)}$$

where τ is $2\pi/\omega$, the period of vibration. The overall rate coefficient is obtained by summing the rate coefficients for each state v weighted by the probability that the ion is in the v^{th} vibrational state, as in Eq.(5b)

$$k \propto \frac{1}{Q_v T_e} \sum_v \frac{e^{-v\theta/T_v}}{(v\,\theta)^{1/2}} \approx \frac{1}{Q_v T_e} \frac{(\pi T_v)^{1/2}}{\theta} \qquad \text{Eq.(20a)}$$

Then approximating Q_v with the harmonic oscillator partition function

$$k \propto \frac{T_v^{1/2}}{T_e} \left(1 - e^{-\theta/T_v}\right) \qquad \text{Eq.(20b)}$$

$$k \xrightarrow[T_v \gg \theta]{} \frac{const}{T_e T_v^{1/2}} \xrightarrow[T_e = T_v = T]{} \frac{const}{T^{3/2}} \qquad \text{Eq.(20c)}$$

At very high temperature the overall rate coefficient is predicted to vary inversely with the electron temperature and inversely with the square root of the vibrational temperature. In many practical cases T_e and T_v will be nearly equal, and if full equilibrium obtains, the overall theoretical rate will vary as $T^{-3/2}$ in accord with the experiments of Dunn and Lordi[25]. The constant is chosen so that at high temperature equilibrium the value will match Dunn and Lordi's measurement, Eq.(15b); then the rate coefficient for dissociative electron recombination with NO^+ is

$$k = 3.0 \times 10^{18} \frac{T_v^{1/2}}{T_e} \left(1 - e^{-3420/T_v} \right) \quad cc/mol\text{-}sec \quad \text{Eq.(21)}$$

The temperatures are in °K. At very high temperature the vibrational partition function and the sum over vibrational states in Eq.(20a) should be truncated and anharmonic effects included. However, since these appear in ratio with one another these corrections will tend to be compensating. Since this reaction is exothermic, the effect of excited electronic species with different vibrational frequencies can be discounted, since the small populations in these excited states have little effect on the total rate observed. Thus Eq.(21) is assumed to be a relatively reliable rate coefficient for the dissociative electron recombination with the NO^+ ion. This function will next be used with the reaction's equilibrium constant to determine the endothermic rate coefficient for ionization resulting from collision of N and O atoms.

IONIZATION DUE TO N + O COLLISION

If the exothermic rate coefficient for NO^+ and electron recombination is known, the endothermic rate for ionization due to collisions between N and O atoms can be obtained by dividing the exothermic rate with the equilibrium constant. However, in the present case, a state of pseudo-equilibrium is considered where the electron temperature, the vibrational temperature, and the heavy particle kinetic temperature are approximately decoupled and frozen. Then the exothermic rate is presumed given by Eq.(21), while the equilibrium constant needs to be evaluated for the pseudo-steady condition rather than at full equilibrium.

A pseudo-steady state of a chemically reacting mixture requires that the change in chemical potential created by the reaction must nearly vanish

$$\Delta\mu = \mu_{NO^+} + \mu_e + \mu_N + \mu_O \approx 0$$

$$= \Delta E^\circ - kT \ln Q(NO^+) - kT_e \ln Q(e) + kT \ln Q(N) + kT \ln Q(O) \qquad \text{Eq.(22a)}$$

where the change in zero point energy is just

$$\Delta E^\circ = E^\circ_{NO^+} - E^\circ_N - E^\circ_O \qquad \text{Eq.(22b)}$$

since the zero point energy of the free electrons is taken as zero. Then

$$\frac{\Delta E^\circ}{kT} = \ln \frac{Q(NO^+)\,[Q(e)]^{T_e/T}}{Q(N)\;Q(O)} \qquad \text{Eq.(23)}$$

This pseudo-steady relation differs from the full equilibrium relation in that the electron partition function is raised to the power T_e/T due to the fact that the electrons have a different kinetic temperature than the heavy particles.

The partition functions can be either pressure standardized or concentration standardized[29]. Since the number of mols is constant in this reaction, the equilibrium constant is the same in either case. The notation $Q_p(i)$ and $Q_c(i)$ will be used for the pressure standardized and concentration standardized partition functions for specie i, respectively.

$$\begin{aligned}\frac{\Delta E^\circ}{kT} &= \ln \frac{Q_p(NO^+)\,[Q_p(e)]^{T_e/T}}{Q_p(N)\;Q_p(O)} - \ln \frac{p_{NO^+}\,[p_e]^{T_e/T}}{p_N\,p_O} \\ &= \ln \frac{Q_c(NO^+)\,[Q_c(e)]^{T_e/T}}{Q_c(N)\;Q_c(O)} - \ln \frac{n_{NO^+}\,[n_e]^{T_e/T}}{n_N\,n_O}\end{aligned} \qquad \text{Eq.(24)}$$

where p_i and n_i are the partial pressures and densities of species i in the chosen standard units (typically atmospheres pressure and either molecules/cc or mol/cc, respectively). In concentration units, the equilibrium constant can be expressed

$$K_{eq} = \frac{n_{NO^+}\,n_e}{n_N\,n_O} = G \cdot \frac{Q_c(NO^+)\;Q_c(e)}{Q_c(N)\;Q_c(O)}\; e^{-\Delta E^\circ/kT} \qquad \text{Eq.(25)}$$

This has the same functional form as the full equilibrium constant except for the correction factor G

$$G = \left(\frac{n_e}{Q_c(e)}\right)^{(1-T_e/T)} \qquad \text{Eq.(26)}$$

which is a function of the electron concentration n_e and the temperature ratio T_e/T. G becomes unity when the kinetic temperatures are equal, of course.

To the first order approximation the upper electronic states are neglected and the diatomic species are considered rigid rotating harmonic oscillators. Then the functional relations of the concentration standardized partition functions are in standard units of mol/cc

$$Q(NO^+) \propto \frac{T^{5/2}}{(1-e^{-\theta/T_v})} \qquad \text{Eq.(27a)}$$

$$Q(e) \propto T_e^{3/2} \qquad \text{Eq.(27b)}$$

$$Q(N) \propto T^{3/2} \qquad \text{Eq.(27c)}$$

$$Q(O) \propto T^{3/2} \qquad \text{Eq.(27d)}$$

To this order, the functional expression for the equilibrium constant is

$$K_c = \frac{k_{endo}}{k_{exo}} \propto G \cdot \frac{T_e^{3/2}}{T^{1/2}\ (1-e^{-\theta/T_v})}\ e^{-\Delta E/kT} \qquad \text{Eq.(28)}$$

and the form for the endothermic rate coefficient becomes

$$k_{endo} = k_{exo}K_c \propto G \cdot \frac{T_v^{1/2}T_e^{1/2}}{T^{1/2}}\ e^{-\Delta E/kT} \qquad \text{Eq.(29)}$$

$$\overline{T_v=T_e=T > \theta} > const\ T^{1/2}\ e^{-\Delta E/kT}$$

The high temperature equilibrium limit is the same relation proposed by Blottner[28] and used by Gupta,et al[3].

The constant of Eq.(29) is determined using quantitative values of the partition functions. Again to first order, neglecting upper electronic states and considering the diatoms as rigid rotator harmonic oscillators, the logarithm of the concentration standardized partition function is for the molecules

$$\ln Q_c = \ln\left(\frac{2\pi mkT}{h^2}\right)^{3/2} + \ln\left(\frac{T}{\theta_r}\right) - \ln(1-e^{-\theta_v/T_v}) + \ln g_o \qquad \text{Eq.(30a)}$$

$$= \frac{5}{2}\ln T + \frac{3}{2}\ln M - 8.0725 - \ln\theta_r - \ln(1-e^{-\theta_v/T_v}) + \ln g_o$$

while for the atoms it is

$$\ln Q_c = \frac{3}{2}\ln T + \frac{3}{2}\ln M - 8.0725 + \ln g_o \qquad \text{Eq.(30a)}$$

where M is the molecular weight in atomic mass units, θ_r the rotational energy constant B/k in degK, θ_v the characteristic vibrational temperature $\hbar\omega/k$ in degK, and g_o the degeneracy of the ground state, or low lying states, of electronic excitation. For the species of interest here the concentration standardized partitions functions in units of mol/cc are

$$\ln Q_c(NO^+) = \frac{5}{2}\ln T - 4.0286 - \ln(1 - e^{-3420/T_v}) \qquad \text{Eq.(31a)}$$

$$\ln Q_c(e) = \frac{3}{2}\ln T_e - 19.3324 \qquad \text{Eq.(31b)}$$

$$\ln Q_c(N) = \frac{3}{2}\ln T - 2.7276 \qquad \text{Eq.(31c)}$$

$$\ln Q_c(O) = \frac{3}{2}\ln T - 1.7164 \qquad \text{Eq.(31d)}$$

and the change in zero point energy is

$$\Delta E^\circ/k = 32400^\circ K \qquad \text{Eq.(31e)}$$

Accordingly, the first order approximation for the equilibrium constant is

$$K = 1.218 \times 10^{-8}\, G \cdot \frac{T_e^{3/2}}{T^{1/2}\,(1 - e^{-3420/T_v})}\, e^{-32400/T} \qquad \text{Eq.(32)}$$

and the endothermic reaction rate which results from multiplying Eq.(28) with Eq.(21) is

$$k_{endo} = 4.8 \times 10^{10}\, G \cdot \frac{T_v^{1/2} T_e^{1/2}}{T^{1/2}}\, e^{-32400/T}\ cc/mol\text{-sec} \qquad \text{Eq.(33)}$$

At high temperature equilibrium this rate approaches

$$k_{endo} \overline{\qquad T_e - T_v - T > \theta} > 4.8 \times 10^{10}\ T^{1/2}\ e^{-32400/T}\ \ cc/mol\text{-}sec \qquad \text{Eq.(34)}$$

For concentration units in mol/cc, the free electron partition function of Eq.(31b) is used and the correction factor G may be expressed

$$\log G = (1 - T_e/T)\left(\log n_e - \frac{3}{2}\log T_e + 8.396\right) \qquad \text{Eq.(35)}$$

Fig.(7) shows the ratio of log G to $(1-T_e/T)$ as a function of electron temperature T_e for electron concentrations of 10^{-5}, 10^{-7}, 10^{-9}, and 10^{-11} mol/cc. The highest density corresponds to about 10% ionization at a total density of one amagat, and the smaller densities correspond to smaller degrees of ionization or to smaller total density at higher altitude, for example.

HIGHER ORDER PARTITION FUNCTIONS

At very high temperature some additional terms in the partition functions become important because the upper electronic states are excited and the effects of vibration-rotation coupling and the anharmonicity of the diatomic species become more significant. Jaffe[30] shows that more rigorous partition functions for these species are duplicated reasonably well by the Dunham potential approximation, for which the rotational-vibrational energy of the diatomic particle is expressed in terms of the quantum numbers j and v respectively

$$E_{vr} = Bj(j+1) - \left(\frac{4B^3}{\omega^2}\right) j^2(j+1)^2 + \omega v - (\omega x) v^2 - \alpha v j(j+1) \qquad \text{Eq.(36)}$$

Note that the older spectroscopic notation is used in Eq.(36), which is sufficiently accurate for the purposes at hand, and that the second rotational energy constant D (no relation to dissociation energy) has been given the value $(4B^3/\omega^2)$ as derived by Pauling and Wilson[31] and Herzberg[32]. The expression for the partition function can be expressed

$$Q = Q_t \sum_i g_i\ e^{-e_i/kT}\ Q_{ri}\ Q_{vi}\ (1+\Gamma_i T) \qquad \text{Eq.(37)}$$

where the factors Q_t, Q_{ri}, and Q_{vi} are the usual separable partition functions for translation, rotation, and vibration respectively.

The summation is over all electronic states i with energy e_i and degeneracy g_i ; Q_{ri} and Q_{vi} come under the summation since the rotational and vibrational constants all depend on the electronic state, but Q_t does not.

Mayer and Mayer[33] derive the factor Γ which corrects the result for vibration-rotation coupling and anharmonicity for the case where the temperatures are all in equilibrium. In the present problem the electronic and vibrational temperatures are taken equal to T_v and rotations are considered to be at equilibrium with the kinetic gas temperature T. The correction factor rederived for this state of nonequilibrium becomes

$$1 + \Gamma_i T = 1 + \left(\frac{8B_i}{\omega_i}\right)\frac{kT}{\hbar\omega_i} + \left(\frac{\alpha_i}{B_i} + \frac{2(\omega x)_i}{\omega_i}\right)\frac{kT_v}{\hbar\omega_i} \qquad \text{Eq.(38a)}$$

The rotational and vibrational constants for the different electronic states have been tabulated in convenient short form by Jaffe[30] and Park[6]. One additional correction that should be included at high temperature is truncation of the rotational and vibrational partition functions at the dissociation energy D so they do not become infinite as they would for and infinity of states. The separable rotational partition function then is

$$Q_{ri} = \frac{kT}{B_i}\left(1 - e^{-D_i/kT}\right) \qquad \text{Eq.(38b)}$$

while the separable vibrational partition function is

$$Q_{vi} = \frac{1 - e^{-D_i/kT_v}}{1 - e^{-\hbar\omega_i/kT_v}} \qquad \text{Eq.(38c)}$$

The ratio of the improved partition function for NO+, Eq.(37), to the first order expression Eq.(30a) is graphed in Fig.(8) for three ratios of vibration-electron temperature to kinetic temperature: 1.0, 0.6, and 0.3. At 50,000°K the more exact partition function can become 5 to 10 times larger than the simplified low temperature expression, though diatomic species may not last long at that temperature, of course.

The large multiplicity of electronic states of the atoms near the ionization limit poses a problem; the partition functions grow to infinity if all the states are included, but the effective cutoff for these states is not so clear. Often the ionization limit is lowered[34] to the level where the free space available to the outer electron is limited by the density of the gas, or by the Debye shielding effect of electrons surrounding the ion which

truncates the range of the ion's Coulomb potential, or by collisions with electrons which broaden the energy levels until they effectively become part of the continuum for the free electron. These criteria are awkward to use because they depend on different properties of the gas mixture[29]; also the cutoffs are generally at such high quantum numbers that the partition functions are still suspiciously large. The table of electronic energy levels for the atoms provided by Park[6] terminates at quantum level 10, which might be sufficiently close to the ionization limit for these almost exactly hydrogen eigenvalues. A simple cutoff will be used here which should apply to the case where the electron density is far below the equilibrium value at least; the upper electronic states within about kT of the ionization limit I will be depleted by rapid escape to the ionized continuum with few reverse reactions to replenish these upper states, leaving a pseudo steady decreased population in these states[35,1]. In order to provide a smooth transition of the upper state populations, the equilibrium distribution is multiplied by an effective cutoff function

$$\frac{n_i}{n} = \left(1 - e^{-(I-e_i)/kT_e}\right) g_i \, e^{-e_i/kT_e} \qquad \text{Eq.(39)}$$

Fig.(8) also shows the calculated ratios of the improved partition functions to the first order functions for the N and O atoms, again for three different ratios T_e/T.

The final correction to the equilibrium constant is the ratio of $Q(NO^+)/Q_o(NO^+)$ to the product of $Q(N)/Q_o(N)$ and $Q(O)/Q_o(O)$ from Fig.(8). This correction factor is shown on Fig.(9). Due to the compensation provided by these ratios, the first order approximation for the equilibrium constant is within a factor of two of the more exact values at full equilibrium; the correction rapidly approaches unity as the vibration electron temperature decreases. In view of the approximations inherent in the model, a further correction of this small amount seems unwarranted.

HEAVY MOLECULE COLLISION IONIZATION OF NO

The ionization of NO by collision with heavy molecules in the gas is so infrequent that this reaction mechanism is usually much less important at high temperature than the collision of N and O atoms, although this reaction is sometimes included in schemes for solving flow of chemically reacting air[3,28]. However, this reaction is particularly interesting in view of the fact that it is one of the rare cases where measured collision cross sections[9,10] can be compared with an accepted rate coefficient.

The cross section function can be expressed

$$\frac{S}{S_o} = \frac{2y}{x} q(1-q) \qquad \text{Eq.(40)}$$

where q is the Landau Zener probability that no transition takes place at the potential crossing region

$$q(y) = e^{-c(x_o/y)^{1/2}} \qquad \text{Eq.(41)}$$

The rate coefficient of Eq.(1) then becomes

$$k_f = \bar{u}\, S_o F(x_o)\, e^{-x_o} \qquad \text{Eq.(42)}$$

where the Arrhenius preexponential factor $F(x_o)$ is

$$F(x_o) = 2 \int_o^\infty q\,(1-q)\; y\, e^{-y}\, dy \qquad \text{Eq.(43)}$$

This integral was performed by numerical quadrature and the results are given in Fig.(10) where the logarithm of $F(x_o)$ is shown as a function of the logarithm of $(c^2 x_o)$. For the NO ionization cross sections shown on Fig.(4), the constant c is about 10. When a reasonably sized total cross section S_o of 10^{-15} cm^2 is used, the resulting rate coefficient is much smaller than the accepted rate coefficient[3,28]

$$k_f = \frac{2.2 \times 10^{15}}{T^{.35}}\, e^{-108000/T} \quad cc/mol\text{-}sec \qquad \text{Eq.(44)}$$

This occurs because the excited states are not included in the computation, as they should be at high temperature. The total rate is a summation over all excited states as in Eq.(5b)

$$k_f = \sum_i k_i \frac{n_i}{n} = \frac{\bar{u} S_o}{Q} \left(\sum_i \frac{g_i\, F_i(x_i)}{(1-e_i/I)^2} \right) e^{-x_o} \qquad \text{Eq.(45)}$$

The cross sections are increased by $(1-e_i/I)^{-2}$, where e_i is the electronic energy of state i, to account for the increased size of the excited state wave function, which in the upper states at least is almost hydrogen like. The summation is approximated for all the electronic, vibrational, and rotational states available to the NO molecule. The resulting ionization rate coefficient is shown by the dashed curve of Fig.(11), where the reference total cross section S_o is chosen 1.6×10^{-15} cm^2 so agreement is achieved at 10000°K. Note that this factor includes the fraction of collisions which approach along the transition potential. The principal point is that the functional dependence predicted by Eq.(45) can be brought into reasonable accord with the simple Arrhenius expression

of Eq.(44). This lends some extra justification for the extrapolation of the Arrhenius function to much higher temperatures.

CONCLUDING REMARKS

The Landau Zener theory of reaction cross section has been used to derive a functional expression for dissociative electron recombination with the NO^+ ion. The rate coefficient is predicted to vary inversely with the electron temperature and the vibrational partition function and directly with the square root of vibrational temperature. At full equilibrium these temperatures equal the kinetic temperature, in which case the rate coefficient varies inversely with the square root of temperature at normal temperatures and inversely with the 3/2 power of temperature at temperatures that are large compared with the characteristic vibrational temperature, $\hbar\omega/k$. This relation is more or less in agreement with most of the experimental determinations made at both normal and high temperatures, whereas the simple $T^{-3/2}$ variation that has usually been used when making flow field calculations is unable to simultaneously describe closely the observations over the entire range of temperature. Since many of the flow fields around the new generation of space vehicles will involve highly nonequilibrium vibrational and electronic distributions, the specific variation of the rate coefficient with each of these temperatures is required. The present model is able to address this need in an approximate manner, at least.

Unfortunately, measurements of cross section are not available for dissociative electron recombination with ions. Thus, comparison with the observed rate coefficient is the only way that the appropriateness of the Landau Zener theory to these reactions can be judged. However, in the case of a reaction of relatively minor importance, heavy particle impact ionization of the NO molecule, measured cross sections are available, at least for the ground or low level vibrational and electronic states of the molecule. The Landau Zener model can be adjusted to fit these measured cross sections reasonably well and then integrated over a Maxwell Boltzmann distribution of collision energies. The resulting rate coefficient applies only to ground state NO and so is much smaller than the total rate coefficient for a gas which includes higher states of the molecule. However, when the excited states are assumed to have the same functional form of cross section and the total scattering size is taken as the size of the outer electron wave function, the summation over all excited states provides a rate coefficient in reasonable accord with the equation that has been used to represent the total rate coefficient for heavy particle collision ionization of NO.

REFERENCES

1. C.F.Hansen: "Rate Processes in Gas Phase", NASA RP1090 (1983)

2. M.Camac and A.Vaughan: J.Chem.Phys. 34, 460 (1961)

3. R.N.Gupta, J.M.Yos, R.A.Thompson, and K.P.Lee: "A Review of Reaction Rates and Thermodynamic and Transport Properties for an 11-Species Model for Chemical and Thermal Nonequilibrium Calculations to 30 000 K", NASA RP1232 (1990)

4. C.F.Hansen: "Dissociation of Diatomic Gases", Final Report on NASA Grant NAS1-1046 with the University of Oregon (1990)

5. C.Lotz: Zeit.fur Physik, 216, 241 (1968)

6. C.Park: "Nonequilibrium Hypersonic Aerothermodynamics", John Wiley, N.Y.(1990)

7. W.L.Fite and R.T.Brackman: Phys.Rev., 112, 1141 (1958)

8. A.C.H.Smith, E.Caplinger, R.Neynaber, E.W.Roth, and S.M. Trujillo: Phys.Rev., 127, 1647 (1962)

9. N.G.Utterback: "Inelastic Molecular Collisions, Rarefied Gasdynamics", Proc.6th Intl.Symp.on Rarefied Gasdynamics, MIT Jul 1968, Academic Press, N.Y.(1969)

10. N.G.Utterback and B.VanZyl: J.Chem.Phys., 68, 2742 (1978)

11. L.Landau: Phys.Z.Sow., 1, 88 (1932): ibid. 2, 46 (1932)

12. C.Zener: Proc.Roy.Soc., A137, 696 (1932); Proc.Camb.Phil. Soc., 29, 136 (1933)

13. S.C.Lin and D.Teare: Phys.Fluids, 6, 355 (1963)

14. J.P.Doering and B.H.Mahan: J.Chem.Phys., 36, 669 (1962)

15. V.A.J.VanLint, J.Perez, M.E.Wyatt, and D.K.Nicholls: Gen. Atomic Rept. RTD-TDR-63-3076 (1963)

16. R.C.Gunton and T.M.Shaw: Phys.Rev., 140, 756 (1965)

17. C.S.Weller and M.A.Biondi: Bull.Am.Phys.Soc., 11, 495 (1966)

18. R.H.Young and G.St.John: Phys.Rev., 152, 25 (1967)

19. R.C.Whitten and I.G.Poppoff: J.Geophys.Res., 66, 2779 (1961)

20. J.Daiber: Bull.Am.Phys.Soc., 9, 585 (1964)

21. W.P.Thompson: Bull.Am.Phys.Soc., 10, 727 (1965)

22. A.Frohm and P.C.T.DeBoer: AIAA J, 5, 261 (1967)

23. K.Branscomb, D.Jenkins, H.I.Schiff, and T.M.Snyder: Ninth Annual Conf. on Mass Spectroscopy, Chicago (1961)

24. R.P.Stein, M.Scheibe, M.W.Syverson, T.M.Shaw, and R.C.Gunton: Phys.Fluids, 7, 1641, (1964)

25. M.G.Dunn and J.A.Lordi: AIAA J, 7, 2099 (1969)

26. C.F.Hansen: Phys.Fluids, 11, 904 (1968)

27. M.H.Bortner: "A Review of Rate Constants of Selected Reactions of Interest in Reentry Flow Fields in the Atmosphere, NBS Tech Note 484 (May 1969)

28. F.G.Blottner: AIAA J, 7, 2281 (1969)

29. R.L.Jaffe: "The Calculation of High Temperature Equilibrium and Nonequilibrium Specific Heat Data for N_2, O_2, and NO", AIAA Paper 87-1633, AIAA 22nd Thermophysics Conf. June 8-10, Honolulu, Hawaii (1987)

30. L.Pauling and E.B.Wilson: "Introduction to Quantum Mechanics", McGraw Hill, N.Y. (1935)

31. G.Herzberg: "Molecular Spectra and Molecular Structure", D.Van Nostrand, N.Y. (1953)

32. J.E.Mayer and M.G.Mayer: "Statistical Mechanics", John Wiley, N.Y. (1957)

33. H.W.Drawin and P.Felenbok: "Data for Plasmas in Local Thermodynamic Equilibrium", Gauthier-Villars, Paris (1965)

34. C.F.Hansen: "Molecular Physics of Equilibrium Gases", NASA SP-3096 (1976)

35. J.Keck and G.Carrier: J.Chem.Phys., 43, 2284 (1965)

* Research supported by the Langley Research Center under Grant NAG-1-1211 with the University of Oregon

** Visiting Professor of Physics, University of Oregon, Eugene, Oregon 97403

Fig.(1) O_2 DISSOCIATION BY Ar COLLISIONS

Fig.(2) SCHEMATIC DIAGRAM OF REACTION POTENTIAL SURFACES

Fig.(3) REACTION CROSS SECTIONS S/S_o AS A FUNCTION OF COLLISION ENERGY E/E_o

Fig.(4) REACTION CROSS SECTION FOR IONIZATION OF GROUND STATE NO BY N_2 COLLISIONS

Fig.(5) EXPERIMENTAL AND THEORETICAL RATE COEFFICIENTS FOR DISSOCIATIVE ELECTRON RECOMBINATION WITH NO^+ IONS

Fig.(6) SCHEMATIC DIAGRAM OF POTENTIAL SURFACES FOR e, NO^+, AND N+O SYSTEMS

Fig.(7) CORRECTION FACTOR FOR EQUILIBRIUM CONSTANT EXPRESSION WHEN APPLIED TO PSEUDO-STEADY NONEQUILIBRIUM ELECTRON TEMPERATURE CONDITIONS

Fig.(8) RATIO OF CORRECTED PARTITION FUNCTIONS TO FIRST ORDER EXPRESSIONS FOR NO^+, N, AND O

Fig.(9) RATIO OF CORRECTED TO FIRST ORDER EXPRESSION FOR THE EQUILIBRIUM CONSTANT OF THE $N + O \rightarrow NO^+ + e$ REACTION

Fig.(10) PREEXPONENTIAL FACTOR FOR LANDAU ZENER RATE COEFFICIENTS

Fig.(11) ENDOTHERMIC RATE COEFFICIENT FOR $NO + N_2 \rightarrow NO^+ + e + N_2$

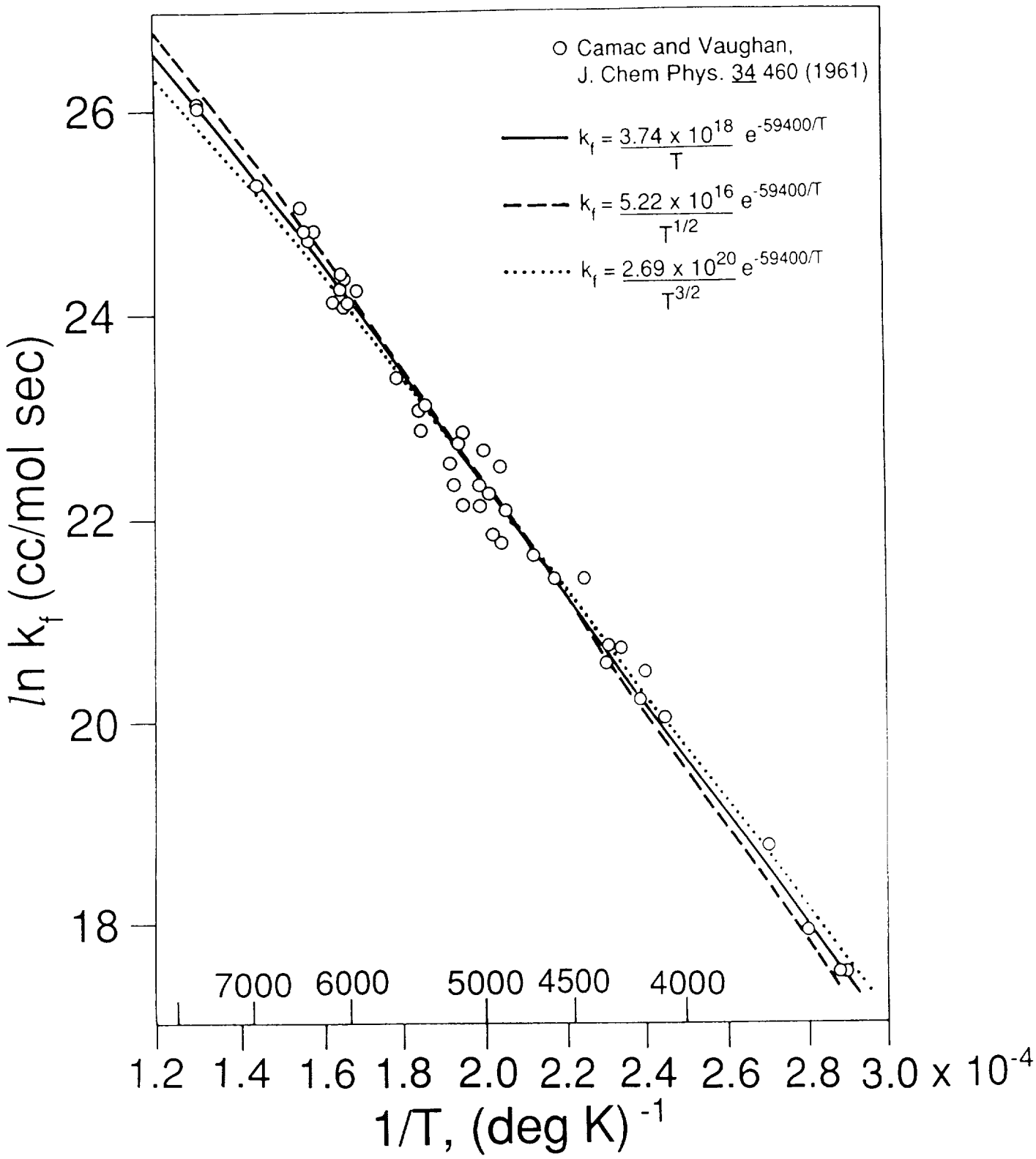

Fig.(1) O_2 DISSOCIATION BY Ar COLLISIONS

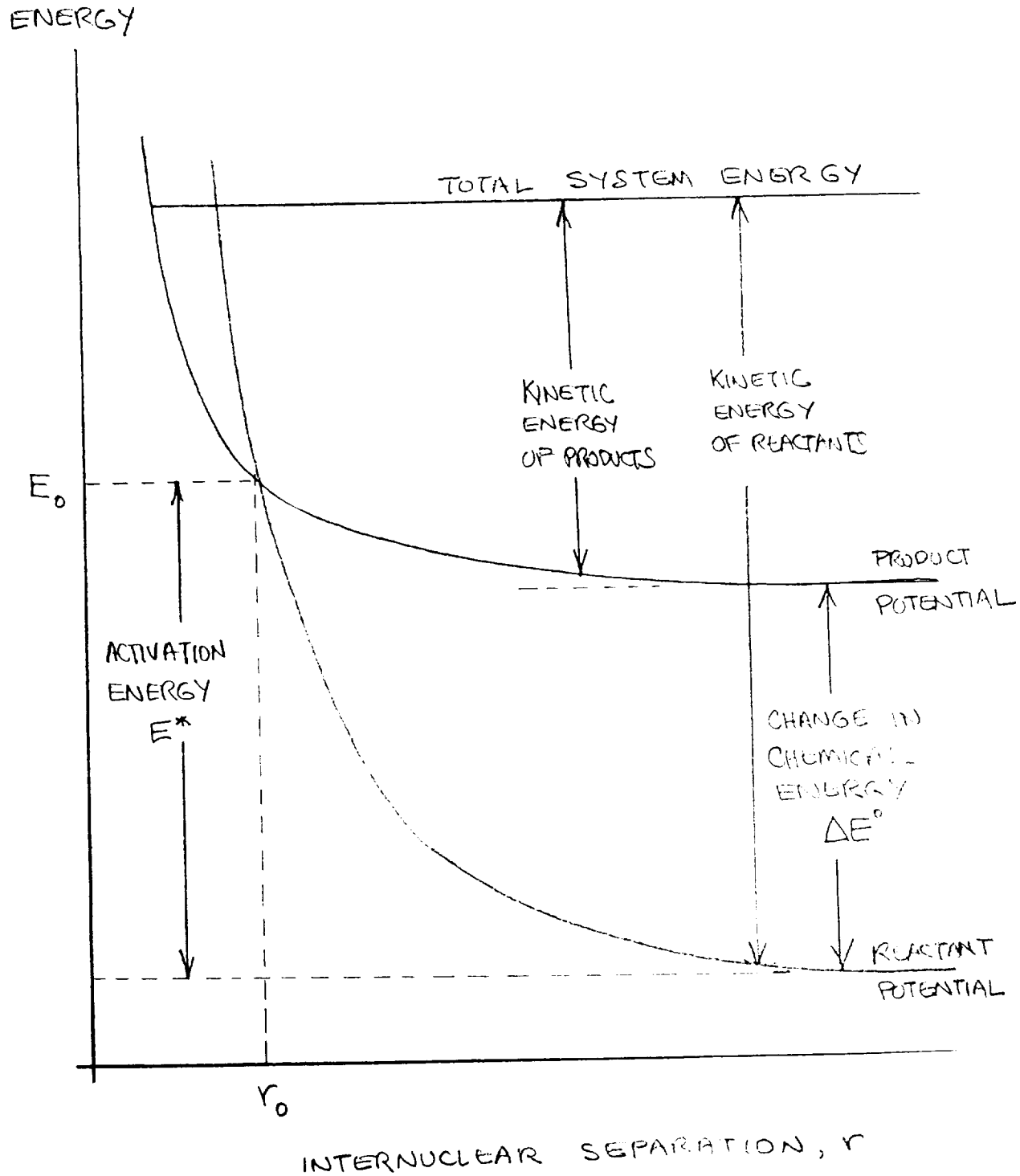

Fig.(2) SCHEMATIC DIAGRAM OF REACTION POTENTIAL SURFACES

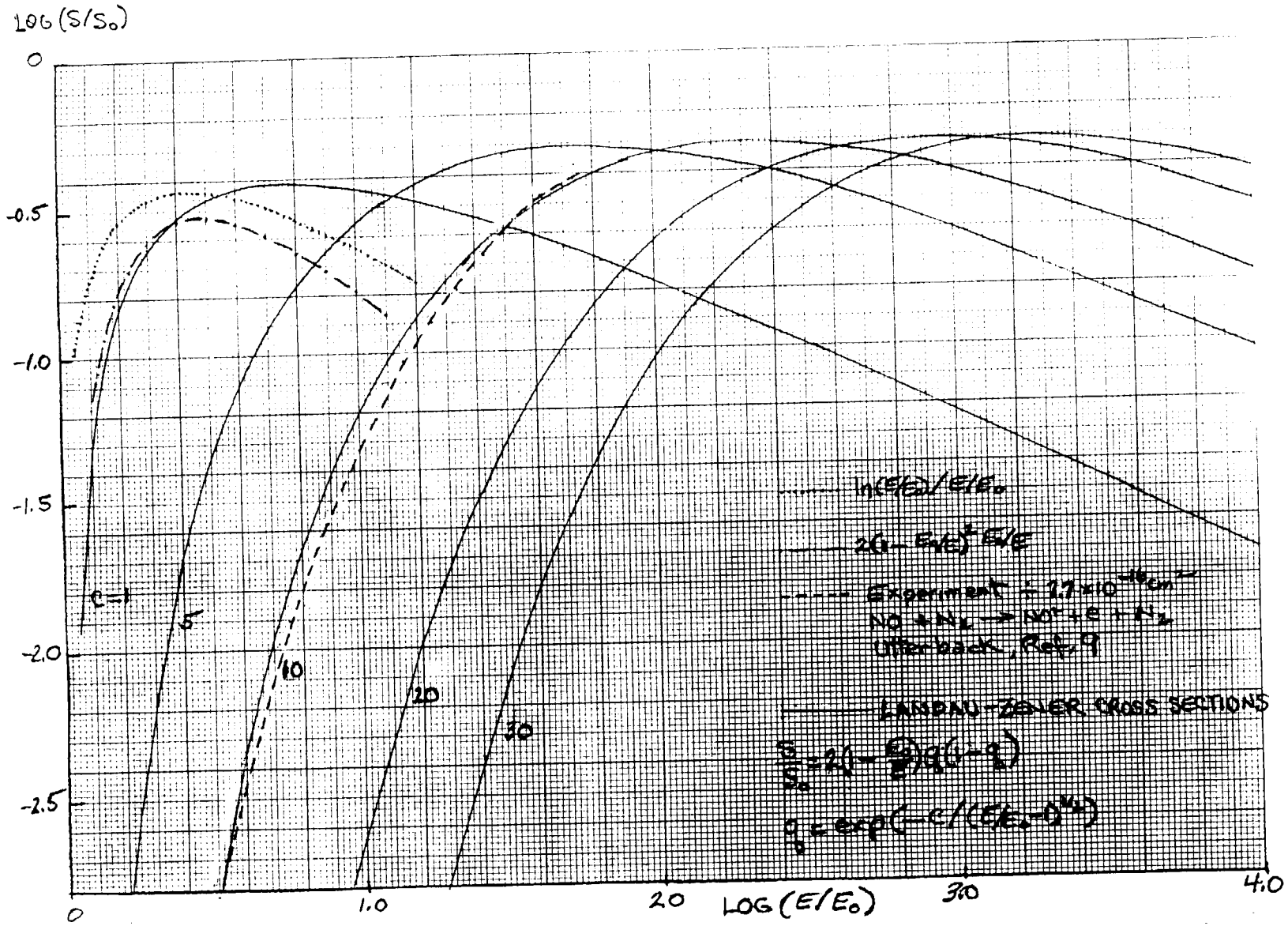

Fig.(3) REACTION CROSS SECTIONS S/S_0 AS A FUNCTION OF COLLISION ENERGY E/E_0

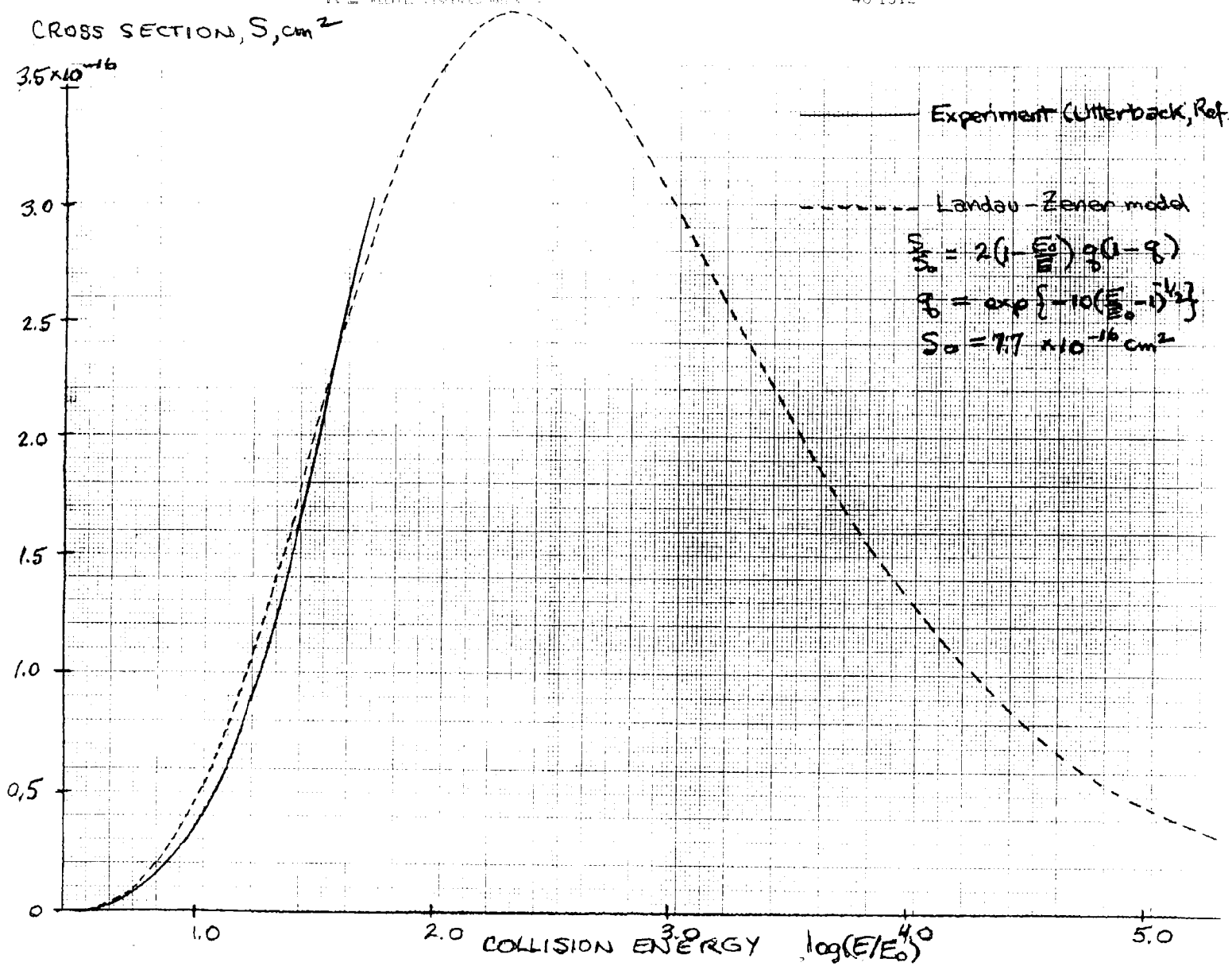

Fig.(4) REACTION CROSS SECTION FOR IONIZATION OF GROUND STATE NO BY N_2 COLLISIONS

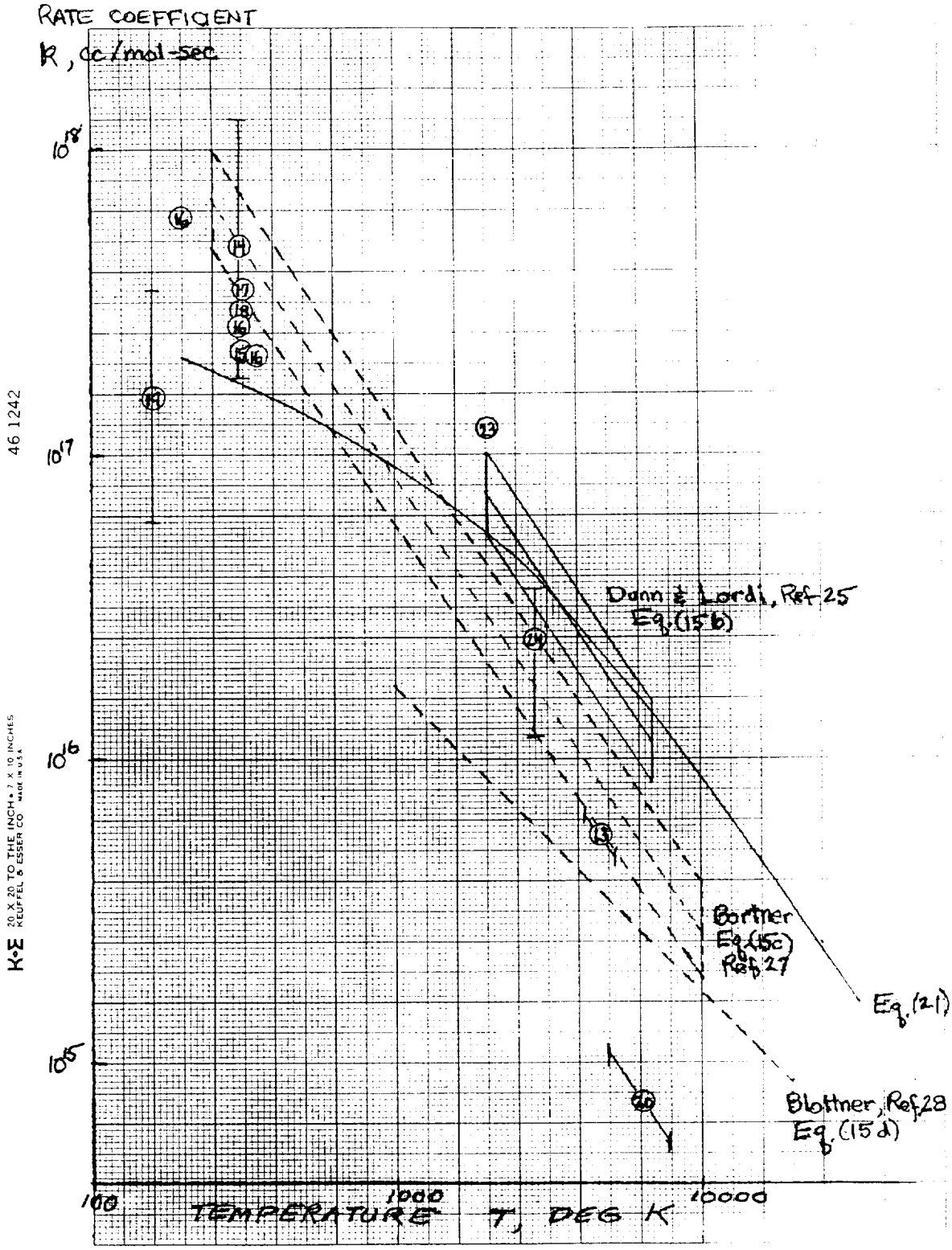

Fig.(5) EXPERIMENTAL AND THEORETICAL RATE COEFFICIENTS FOR DISSOCIATIVE ELECTRON RECOMBINATION WITH NO^+ IONS

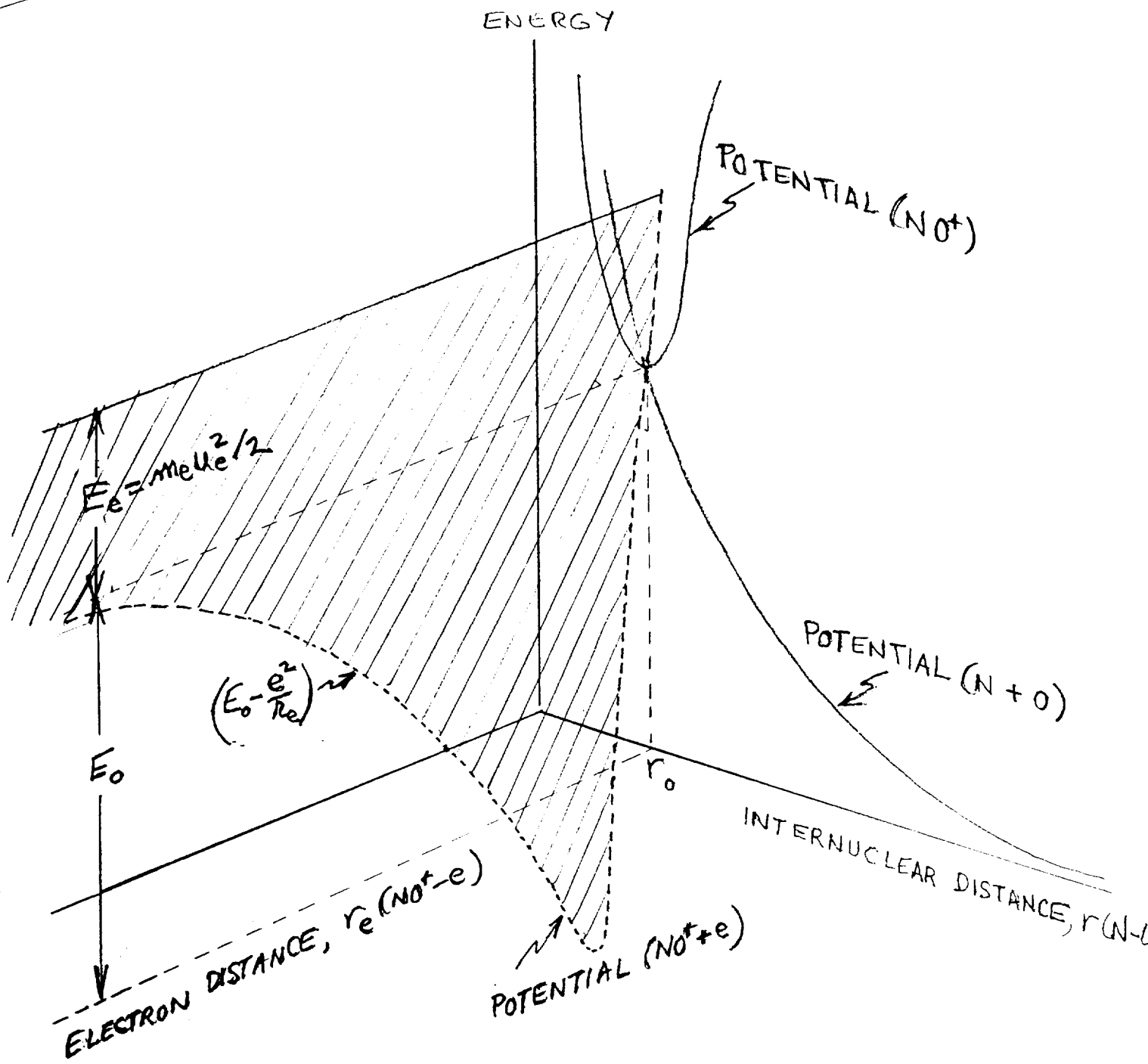

Fig.(6) SCHEMATIC DIAGRAM OF POTENTIAL SURFACES FOR e, NO^+, AND N+O SYSTEMS

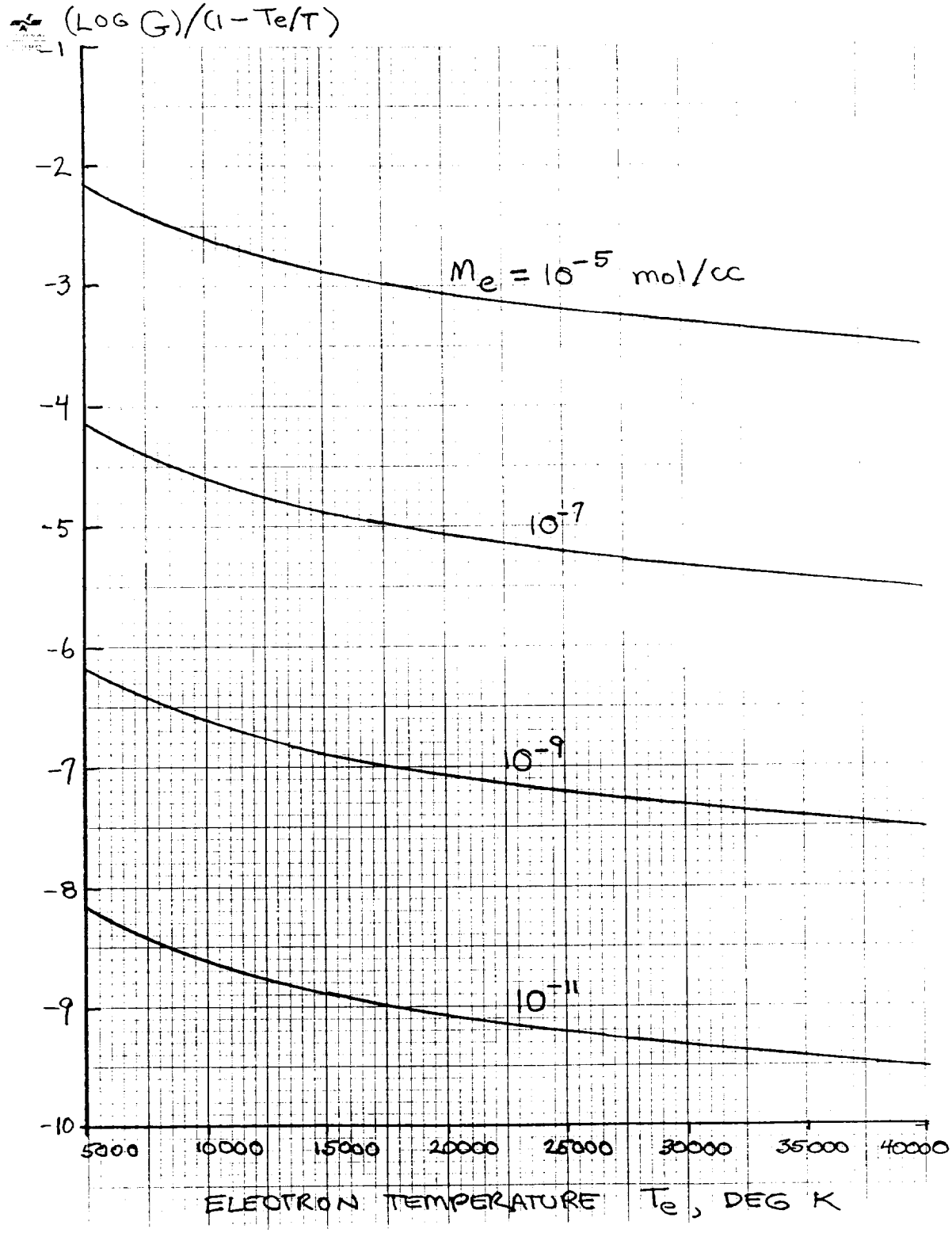

Fig.(7) CORRECTION FACTOR FOR EQUILIBRIUM CONSTANT EXPRESSION WHEN APPLIED TO PSEUDO-STEADY NONEQUILIBRIUM ELECTRON TEMPERATURE CONDITIONS

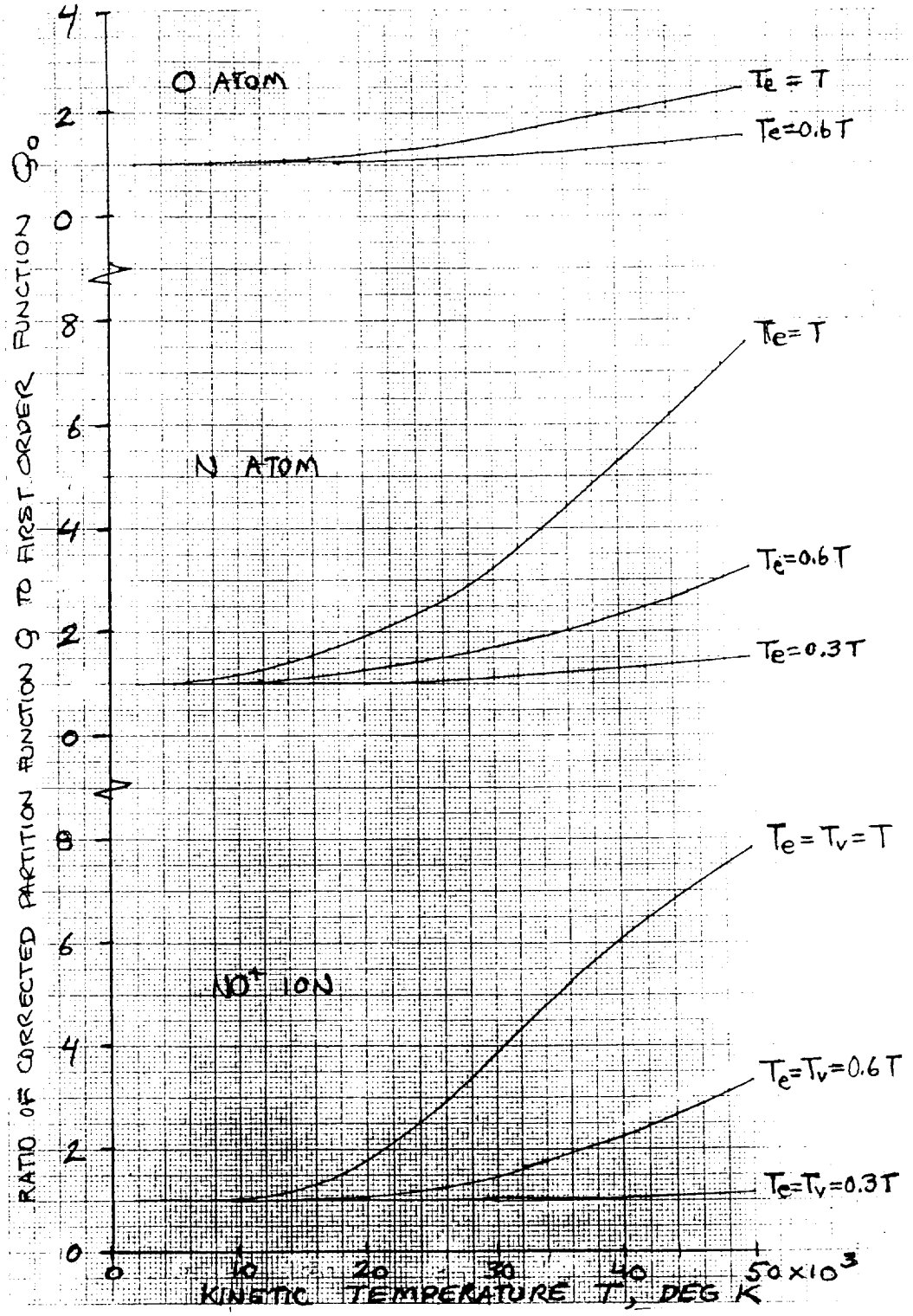

Fig.(8) RATIO OF CORRECTED PARTITION FUNCTIONS TO FIRST ORDER EXPRESSIONS FOR NO^+, N, AND O

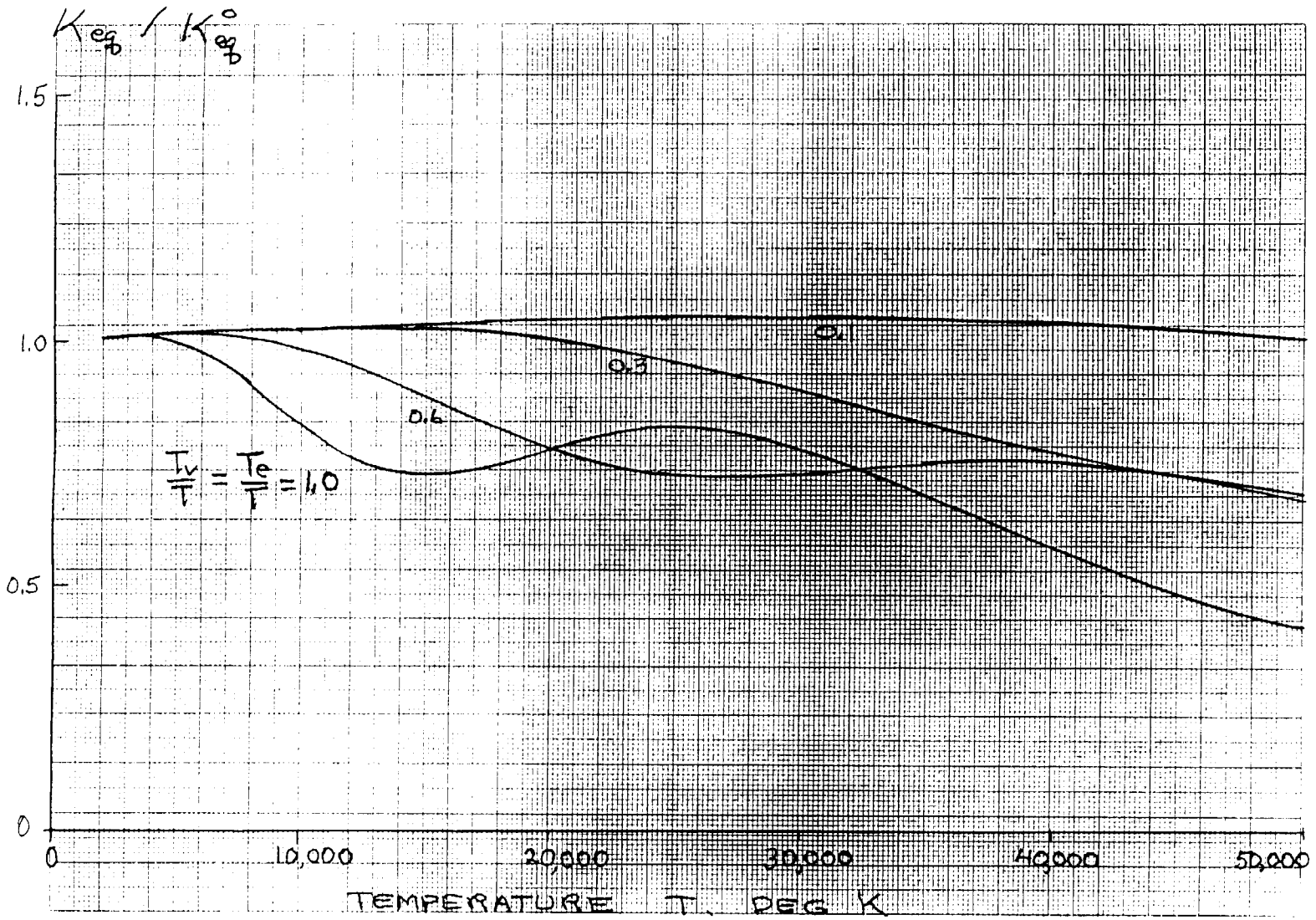

Fig.(9) RATIO OF CORRECTED TO FIRST ORDER EXPRESSION FOR THE EQUILIBRIUM CONSTANT OF THE N + O → NO^+ + e REACTION

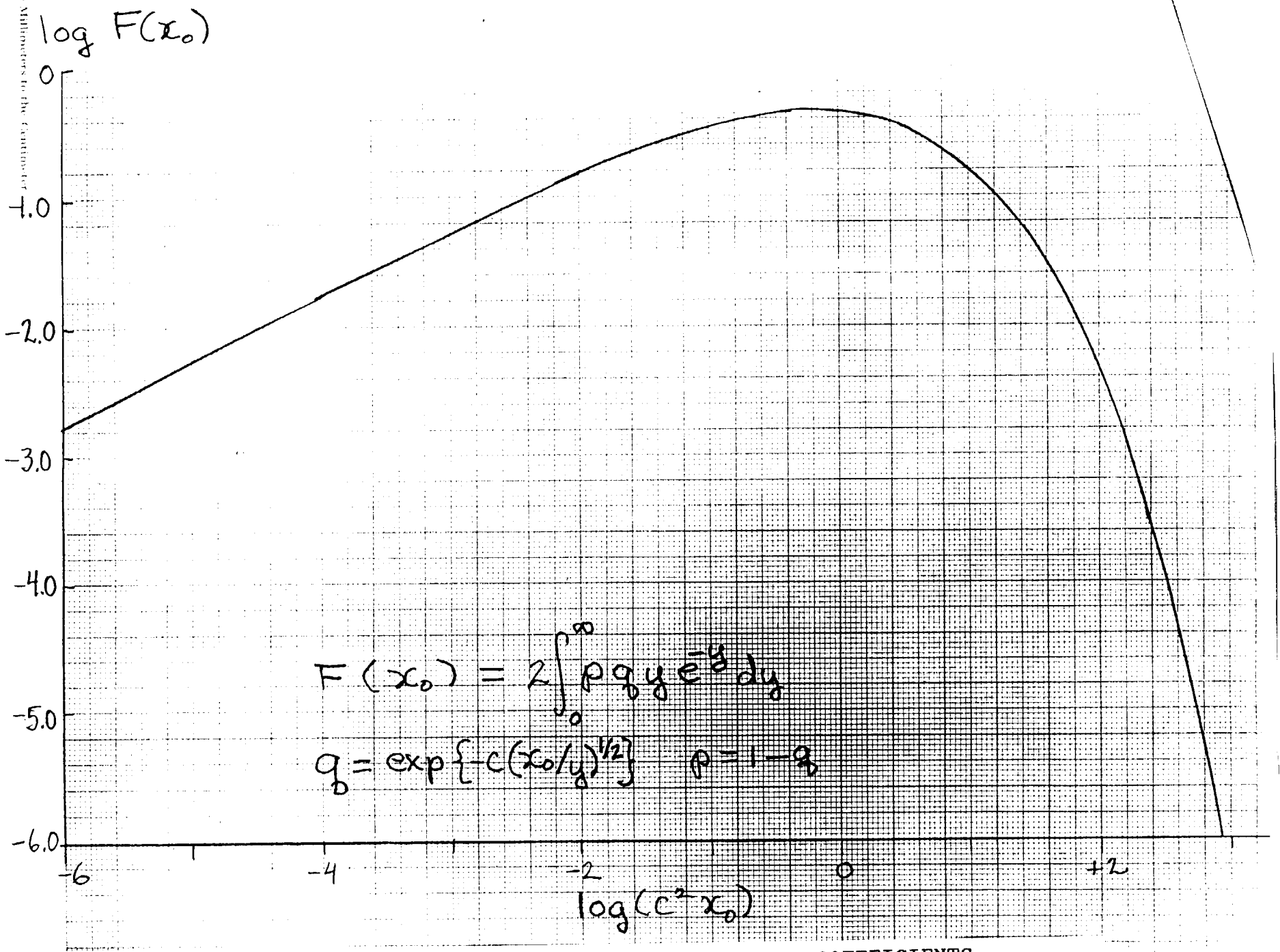

Fig.(10) PREEXPONENTIAL FACTOR FOR LANDAU ZENER RATE COEFFICIENTS

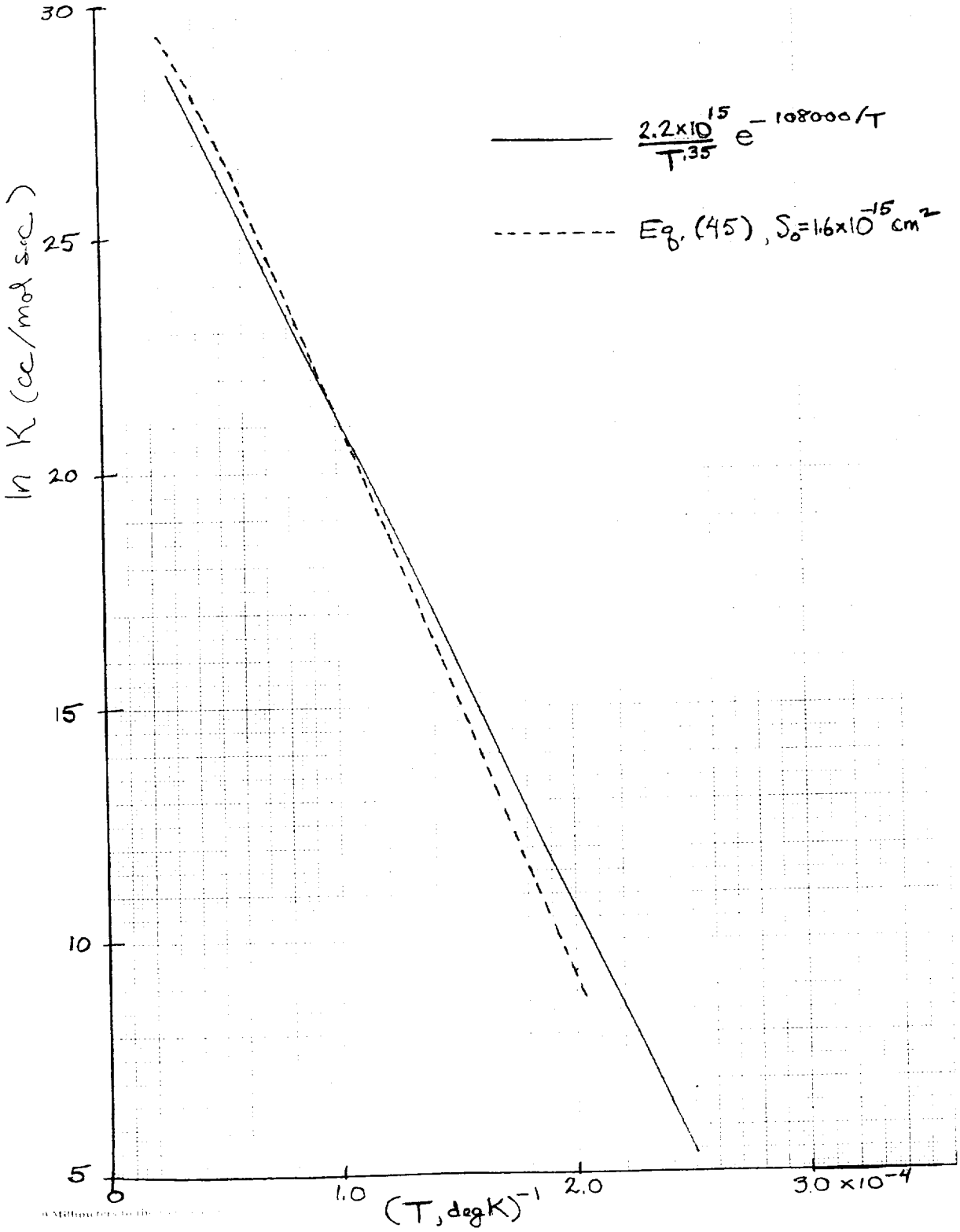

Fig.(11) ENDOTHERMIC RATE COEFFICIENT FOR $NO + N_2 \rightarrow NO^+ + e + N_2$